Published in final edited form as:

Toxicon. 2016 September 15; 120: 57–60. doi:10.1016/j.toxicon.2016.07.017.

Gambierol and n-alkanols inhibit *Shaker* Kv channel via distinct binding sites outside the K^+ pore

Evelyn Martínez-Morales[a,1], **Ivan Kopljar**[a,1,2], **Jon D. Rainier**[b], **Jan Tytgat**[c], **Dirk J. Snyders**[a], **Alain J. Labro**[a,*]

[a]Department of Biomedical Sciences, University of Antwerp, 2610 Antwerp, Belgium

[b]Department of Chemistry, University of Utah, 315 South 1400 East, Salt Lake City, UT 84112-0850, USA

[c]Toxicology & Pharmacology, Campus Gasthuisberg, Onderwijs en Navorsing 2, Herestraat 49, bus 922, KULeuven, B-3000, Belgium

Abstract

The marine polycyclic-ether toxin gambierol and 1-butanol (n-alkanol) inhibit *Shaker*-type K_v channels by interfering with the gating machinery. Competition experiments indicated that both compounds do not share an overlapping binding site but gambierol is able to affect 1-butanol affinity for *Shaker* through an allosteric effect. Furthermore, the *Shaker*-P475A mutant, which inverses 1-butanol effect, is inhibited by gambierol with nM affinity. Thus, gambierol and 1-butanol inhibit *Shaker*-type K_v channels via distinct parts of the gating machinery.

Keywords

Potassium channel; Gating modifier; Lipophilic marine toxin; 1-Alcohol; Electrophysiology

1. K_v channels have drug/toxin binding sites outside the K^+ pore

Voltage-gated K^+ (K_v) channels are tetramers composed of α-subunits with six transmembrane segments S1–S6 (Long et al., 2005a). The S5–S6 segments assemble into the K^+ pore with a gate in the C-terminal region of S6 (Labro and Snyders, 2012). The S1–S4 segments form the voltage-sensing domains (VSDs) that move upon changes in the membrane potential (Long et al., 2005b; Bezanilla, 2000). An interaction between the S4–S5 linker and C-terminal region of S6 creates the electro-mechanical coupling that translates

*Corresponding author. Laboratory for Molecular Biophysics, Physiology and Pharmacology, Department of Biomedical Sciences, University of Antwerp, Universiteitsplein 1, CDE T5.51 2610 Antwerp, Belgium. alain.labro@uantwerpen.be (A.J. Labro).

[1]Both authors contributed equally.

[2]Current address: Discovery Sciences, Janssen Research and Development, 2340 Beerse, Belgium.

Ethical statement

Hereby, we state that the performed research and the work considered for publication complies with the ethical guidelines of Elsevier's policy for journal publication, and to the best of our knowledge we did not violate the ethics in publishing.

Transparency document

Transparency document related to this article can be found online at http://dx.doi.org/10.1016/j.toxicon.2016.07.017.

VSD movements into gate opening/closure (Blunck and Batulan, 2012). The ensemble of regions underlying voltage-dependent channel opening is termed the gating machinery.

Toxins and drugs can potentiate or inhibit K_v channels, which can have a therapeutic potential (Wulff et al., 2009). Gambierol is a polycyclic-ether toxin (MW = 757 g/mol) produced by the marine dinoflagellate *Gambierdiscus toxicus* and is related to ciguatoxins associated with ciguatera food poisoning (Lewis, 2006). Gambierol is a potent inhibitor of K_v1 and K_v3 channels (Cuypers et al., 2008; Kopljar et al., 2009), and has been shown to inhibit K^+ currents in native tissues (Ghiaroni et al., 2005; Schlumberger et al., 2010; Alonso et al., 2012; Perez et al., 2012; Cao et al., 2014). Gambierol most likely operates via a lipid accessible space located between the VSD and the lipid facing side of the pore forming S5 and S6 segments (Kopljar et al., 2009, 2016), a binding site that may correspond with that of the Psora-4 compound (Marzian et al., 2013). Similarly, n-alkanols such as 1-butanol (1-BuOH) act outside the K^+ pore affecting the electro-mechanical coupling (Barber et al., 2011; Bhattacharji et al., 2006; Zhang et al., 2013). Here we report that the *Shaker* channel, the prototypical K_v channel for exploring the gating mechanism, is sensitive to gambierol and show that gambierol and 1-BuOH target different parts of the gating machinery.

2. Gambierol and 1-BuOH do not compete as inhibitors of the *Shaker*-IR K_v channel

Gambierol-sensitive K_v1 and K_v3 channels contain an important threonine residue in S6 (Kopljar et al., 2009), which is conserved in *Shaker* (T469). Therefore, we expected the *Shaker* channel to be sensitive. In this study we used the fast inactivation removed *Shaker*-IR channel, which was transiently expressed in HEK293 cells and whole-cell ionic currents were recorded with the patch-clamp technique (20 h after transfection). Patch-clamp setup and data acquisition/analysis were similar as described previously (Martinez-Morales et al., 2015). During recordings the cells were continuously superfused with a bath solution (in mM): NaCl 130, KCl 4, $CaCl_2$ 1.8, $MgCl_2$ 1, HEPES 10, Glucose 10, adjusted to pH 7.35 with NaOH. The intracellular patch-pipette solution contained: KCl 110, K_4BAPTA 5, K_2ATP 5, $MgCl_2$ 1, HEPES 10, adjusted to pH 7.2 with KOH. Application of 300 nM gambierol to *Shaker*-IR resulted indeed in approximately 80% current inhibition (Fig. 1A). This observation differs from a previous study, which used *Xenopus* oocytes as expression system, reporting *Shaker* to be less sensitive (Cuypers et al., 2008). Since gambierol is highly lipophilic the use of HEK293 cells instead of *Xenopus* oocytes is a likely explanation for the different response. Similarly, $K_v1.2$'s gambierol affinity depends on the expression system used (Konoki et al., 2015).

A valine substitution for T469 reduced, as expected, gambierol sensitivity (Fig. 1B–C). However, this *Shaker*-IR-T469V mutant was still inhibited by 1-BuOH suggesting that both compounds have different binding determinants. To investigate this further, we performed competition experiments and compared the experimental data with the predicted level of inhibition using an allotopic (non-competing) or syntopic (competing) binding model (Jarvis and Thompson, 2013). Experiments were done with concentrations near the IC_{50} values as in these conditions the largest difference between both models is expected; thus we used 50

mM 1-BuOH and 100 nM gambierol, respectively. Both compounds were applied to the cells using a pressurized perfusion system as described previously (Kopljar et al., 2009; Martinez-Morales et al., 2015). For each experiment (number of cells analyzed $n = 7$), we determined first the amount of current inhibition by 50 mM 1 BuOH (58.0 ± 2.6%) and 100 nM gambierol (58.5 ± 3.0%) alone. Subsequently, after reaching steady-state gambierol inhibition, we tested the effect of both compounds combined and applied a mixture of 100 nM gambierol +50 mM 1-BuOH. This mixture yielded a total inhibition of 78.0 ± 2.0% (Fig. 1D–E). The predicted inhibition of the mixture ($I_{NB,G}$) according to the allotopic and syntopic model was calculated using the formulas described by Jarvis and Thompson (2013): $I_{NB,G} = (I_{NB} + I_{NG} - I_{NB}I_{NG})$ and $I_{NB,G} = ((I_{NB} + I_{NG} - 2I_{NB}I_{NG})/(1 - I_{NB}I_{NG}))$, respectively. I_{NB} and I_{NG} were the experimentally determined level of channel inhibition by 1-BuOH and gambierol alone. When both compounds share the same binding site (syntopic model), 73.8 ± 1.7% of inhibition was expected. If both compounds have different binding sites (allotopic model) there would be no competition and 82.4 ± 1.8% of inhibition was expected. Hence, our experimentally observed inhibition differed significantly from both models (Fig. 1E). According to Jarvis and Thompson (2013), this result indicates that gambierol and 1-BuOH possess distinct binding determinants, but binding of gambierol results in a reduced affinity for 1-BuOH most likely through an allosteric effect. The effect of 1-BuOH binding on subsequent gambierol affinity (i.e. establishing first steady-state 1-BuOH inhibition followed by adding the mixture) could not be tested because gambierol unbinding is very slow (Kopljar et al., 2013) and it is important to determine the level of inhibition for both compounds independently when comparing the data with both binding models (Jarvis and Thompson, 2013). To validate our results we performed competition experiments between 1-BuOH and 1-hexanol (1-HeOH) that should compete for the same binding site. Indeed, the experimentally obtained inhibition matched the predicted value of a syntopic model and differed only statistically from that of an allotopic one (Fig. 1F–G).

3. The *Shaker*–IR-P475A pore mutant is inhibited by gambierol

To investigate gambierol's mechanism of action further and to strengthen that gambierol and 1-BuOH affect different parts of the gating machinery, the *Shaker*-IR-P475A mutant was tested for its sensitivity to gambierol. Previously, we reported that this mutation renders *Shaker* insensitive to the well-studied gating modifying compound 4-aminopyridine (4-AP) and inverses the response to n-alkanols such that *Shaker*-IR-P475A's current amplitude is potentiated by 1-BuOH instead of being inhibited (Martinez-Morales et al., 2015). Applying 300 nM gambierol to *Shaker*-IR-P475A yielded 83 ± 4% ($n = 4$) current inhibition at +90 mV, indicating that the mutant displayed a similar gambierol affinity as wild-type *Shaker*-IR (Fig. 2A–C). Fig. 2D shows that the inhibition by gambierol was voltage-independent. Fitting the remaining current activation at +90 mV with a single exponential function yielded a τ_{ac} time constant of 455 ± 15 ms ($n = 4$), which was similar to τ_{ac} in control conditions (573 ± 68 ms, $n = 4$). Fitting the current deactivation at −20 mV yielded τ_{deac} constants of 193 ± 16 ms ($n = 4$) and 197 ± 30 ms ($n = 4$) for control and presence of 300 nM gambierol, respectively. Thus, gambierol did not affect the kinetics of the remaining currents nor the voltage dependence of channel activation since the normalized conductance versus voltage (GV) curves of the remaining currents were similar to the GV curves

obtained in control conditions (Fig. 2E). Thus, in contrast to the potentiating effect of 1-BuOH (n-alkanols) on this mutant (Martinez-Morales et al., 2015), *Shaker*-IR-P475A was still inhibited by gambierol.

4. Gambierol and 1-BuOH have distinct binding sites

Our competition and mutagenesis experiments suggest that gambierol and 1-BuOH act at different binding sites but both compounds affect each other's binding in an allosteric manner. There are several mechanisms to achieve this; a likely possibility is that a conformational change in the electro-mechanical coupling upon gambierol binding subsequently impairs the binding of 1-BuOH. When K_v channels traverse the activation sequence from a closed to an open gate conformation, they pass different intermediate closed states before reaching an activated state from which they transition to the open state in a voltage-independent manner (Fig. 2F). Whereas 1-BuOH traps the channels in the activated state (Martinez-Morales et al., 2015), gambierol stabilizes the channel in an early closed state (Kopljar et al., 2013). If this closed state has a lower 1-BuOH affinity, then gambierol binding would reduce 1-BuOH affinity by locking the channels in this closed (lower affinity) state. Likewise, since the P475A mutation affects only the transition from the activated to the open state (Martinez-Morales et al., 2014), the early closed states are unaffected and the *Shaker*-IR-P475A mutant remains sensitive to gambierol. In conclusion, the toxin gambierol and 1-BuOH interfere with the gating machinery differently by acting via distinct binding sites outside the K^+ pore.

Acknowledgments

This work was supported by the Mexican National Council for Science and Technology CONACyT #203936 (to E.M.M.), the Belgian Research Fund Flanders (FWO – Fonds voor Wetenschappelijk Onderzoek Vlaanderen) grants G.0433.12 (to D.J.S. & J.T) and G0E3414N (to J.T.), and J.T. was supported by funding from IUAP 7/10 (Inter-University Attraction Poles Program, Belgian State, Belgian science Policy).

References

Alonso E, Fuwa H, Vale C, Suga Y, Goto T, Konno Y, Sasaki M, LaFerla FM, Vieytes MR, Gimenez-Llort L, Botana LM. 2012; Design and synthesis of skeletal analogues of gambierol: attenuation of amyloid-beta and tau pathology with voltage-gated potassium channel and N-methyl-d-aspartate receptor implications. J. Am. Chem. Soc. 134:7467–7479. [PubMed: 22475455]

Barber AF, Liang Q, Amaral C, Treptow W, Covarrubias M. 2011; Molecular mapping of general anesthetic sites in a voltage-gated ion channel. Biophys. J. 101:1613–1622. [PubMed: 21961587]

Bezanilla F. 2000; The voltage sensor in voltage-dependent ion channels. Physiol. Rev. 80:555–592. [PubMed: 10747201]

Bhattacharji A, Kaplan B, Harris T, Qu X, Germann MW, Covarrubias M. 2006; The concerted contribution of the S4–S5 linker and the S6 segment to the modulation of a Kv channel by 1-alkanols. Mol. Pharmacol. 70:1542–1554. [PubMed: 16887933]

Blunck R, Batulan Z. 2012; Mechanism of electromechanical coupling in voltage-gated potassium channels. Front. Pharmacol. 3:166. [PubMed: 22988442]

Cao Z, Cui Y, Busse E, Mehrotra S, Rainier JD, Murray TF. 2014; Gambierol inhibition of voltage-gated potassium channels augments spontaneous Ca2+ oscillations in cerebrocortical neurons. J. Pharmacol. Exp. Ther. 350:615–623. [PubMed: 24957609]

Cuypers E, Abdel-Mottaleb Y, Kopljar I, Rainier JD, Raes AL, Snyders DJ, Tytgat J. 2008; Gambierol, a toxin produced by the dinoflagellate *Gambierdiscus toxicus*, is a potent blocker of voltage-gated potassium channels. Toxicon. 51:974–983. [PubMed: 18313714]

Ghiaroni V, Sasaki M, Fuwa H, Rossini GP, Scalera G, Yasumoto T, Pietra P, Bigiani A. 2005; Inhibition of voltage-gated potassium currents by gambierol in mouse taste cells. Toxicol. Sci. 85:657–665. [PubMed: 15689421]

Jarvis GE, Thompson AJ. 2013; A golden approach to ion channel inhibition. Trends Pharmacol. Sci. 34:481–488. [PubMed: 23972927]

Konoki K, Suga Y, Fuwa H, Yotsu-Yamashita M, Sasaki M. 2015; Evaluation of gambierol and its analogs for their inhibition of human Kv1.2 and cytotoxicity. Bioorg. Med. Chem. Lett. 25:514–518. [PubMed: 25556093]

Kopljar, I; Grottesi, A; de, BT; Rainier, JD; Tytgat, J; Labro, AJ; Snyders, DJ. Voltage-sensor conformation shapes the intra-membrane drug binding site that determines gambierol affinity in Kv channels. Neuropharmacology. 2016.

Kopljar I, Labro AJ, Cuypers E, Johnson HW, Rainier JD, Tytgat J, Snyders DJ. 2009; A polyether biotoxin binding site on the lipid-exposed face of the pore domain of Kv channels revealed by the marine toxin gambierol. Proc. Natl. Acad. Sci. U.S.A. 106:9896–9901. [PubMed: 19482941]

Kopljar I, Labro AJ, de Block T, Rainier JD, Tytgat J, Snyders DJ. 2013; The ladder-shaped polyether toxin gambierol anchors the gating machinery of Kv3.1 channels in the resting state. J. Gen. Physiol. 141:359–369. [PubMed: 23401573]

Labro AJ, Snyders DJ. 2012; Being flexible: the voltage-controllable activation gate of kv channels. Front. Pharmacol. 3:168. [PubMed: 22993508]

Lewis RJ. 2006; Ciguatera: Australian perspectives on a global problem. Toxicon. 48:799–809. [PubMed: 16930661]

Long SB, Campbell EB, MacKinnon R. 2005a; Crystal structure of a mammalian voltage-dependent *Shaker* family K^+ channel. Science. 309:897–903. [PubMed: 16002581]

Long SB, Campbell EB, MacKinnon R. 2005b; Voltage sensor of Kv1.2: structural basis of electromechanical coupling. Science. 309:903–908. [PubMed: 16002579]

Martinez-Morales E, Kopljar I, Snyders DJ, Labro AJ. 2015; Alkanols inhibit voltage-gated K(+) channels via a distinct gating modifying mechanism that prevents gate opening. Sci. Rep. 5:17402. [PubMed: 26616025]

Martinez-Morales E, Snyders DJ, Labro AJ. 2014; Mutations in the S6 gate isolate a late step in the activation pathway and reduce 4-AP sensitivity in *shaker* Kv channel. Biophys. J. 106:134–144. [PubMed: 24411245]

Marzian S, Stansfeld PJ, Rapedius M, Rinne S, Nematian-Ardestani E, Abbruzzese JL, Steinmeyer K, Sansom MS, Sanguinetti MC, Baukrowitz T, Decher N. 2013; Side pockets provide the basis for a new mechanism of Kv channel-specific inhibition. Nat. Chem. Biol. 9:507–513. [PubMed: 23728494]

Perez S, Vale C, Alonso E, Fuwa H, Sasaki M, Konno Y, Goto T, Suga Y, Vieytes MR, Botana LM. 2012; Effect of gambierol and its tetracyclic and heptacyclic analogues in cultured cerebellar neurons: a structure-activity relationships study. Chem. Res. Toxicol. 25:1929–1937. [PubMed: 22894724]

Schlumberger S, Ouanounou G, Girard E, Sasaki M, Fuwa H, Louzao MC, Botana LM, Benoit E, Molgo J. 2010; The marine polyether gambierol enhances muscle contraction and blocks a transient K^+ current in skeletal muscle cells. Toxicon. 56:785–791. [PubMed: 20540957]

Wulff H, Castle NA, Pardo LA. 2009; Voltage-gated potassium channels as therapeutic targets. Nat.Rev. Drug Discov. 8:982–1001. [PubMed: 19949402]

Zhang J, Qu X, Covarrubias M, Germann MW. 2013; Insight into the modulation of Shaw2 Kv channels by general anesthetics: structural and functional studies of S4–S5 linker and S6 C-terminal peptides in micelles by NMR. Biochim. Biophys. Acta. 1828:595–601. [PubMed: 23031574]

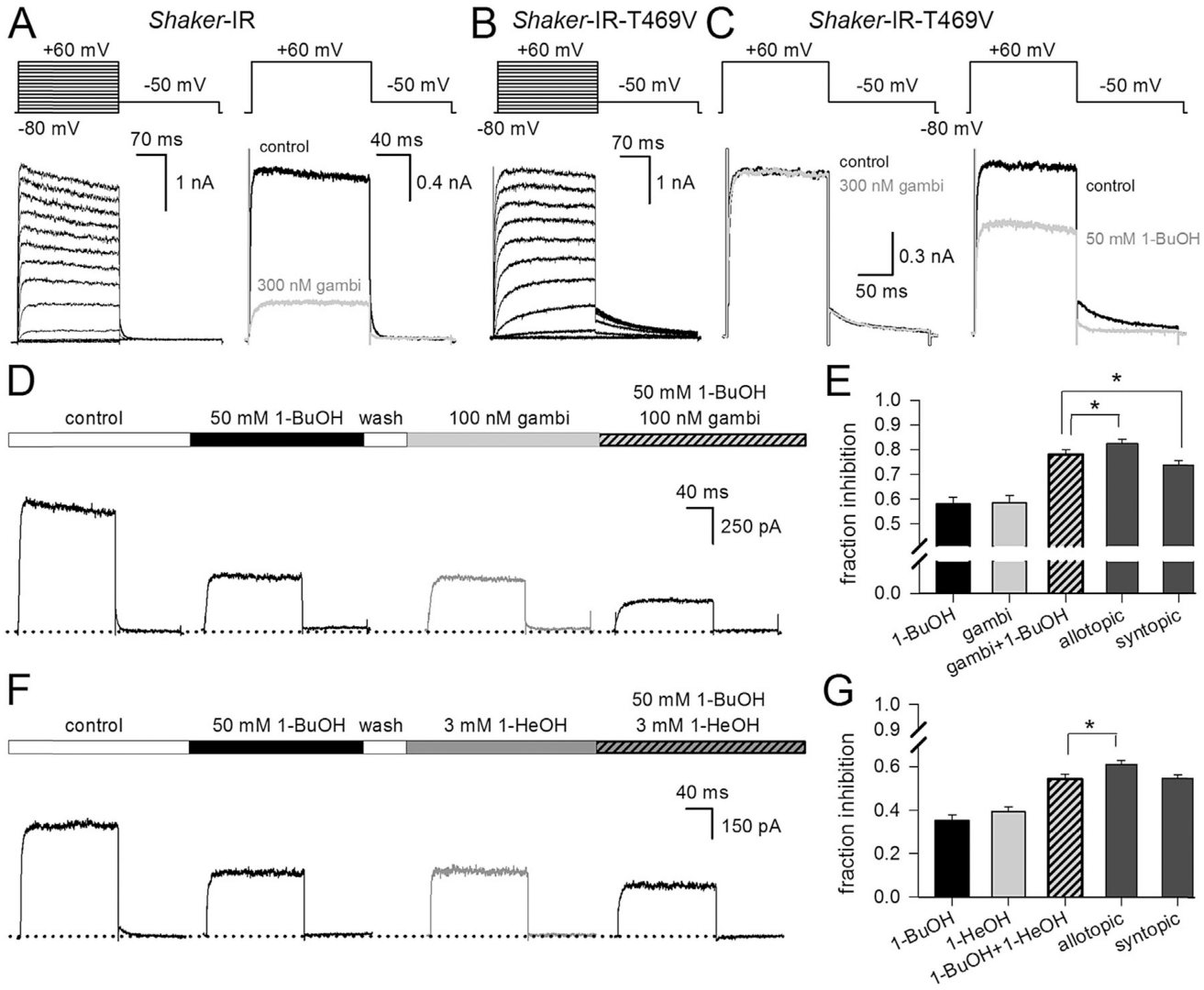

Fig. 1.

Gambierol and 1-BuOH do not compete for inhibiting *Shaker*-IR. **A**, Left, ionic currents of *Shaker*-IR channels recorded at 22 °C and elicited with the pulse protocol shown on top. Right, currents of *Shaker*-IR in control conditions (black trace) and upon steady-state inhibition by 300 nM gambierol (gambi, gray trace). **B**, Representative currents of the *Shaker*-IR-T469V mutant elicited with the pulse protocol shown on top. **C**, Steady-state currents of *Shaker*-IR-T469V in control conditions (black trace) and upon application of either 300 nM gambierol (left recordings, gray trace) or 50 mM 1-BuOH (right recordings, gray trace). **D**, Sequentially recorded steady-state currents of *Shaker*-IR elicited by applying a 150 ms long +40 mV depolarization from a holding potential of −80 mV. After the depolarizing step the membrane potential was briefly repolarized to −45 mV to elicit a deactivating tail current. To reach steady-state conditions, depolarizations were repetitively applied with an inter-pulse interval of 10 s. The bar on top illustrates the sequential addition of 1-BuOH and/or gambierol. Below, representative currents recorded from left to right: in control conditions, upon steady-state inhibition by 50 mM 1-BuOH, steady-state inhibition by 100 nM gambierol after washout of 1-BuOH, and finally the current inhibition by the

mixture (100 nM gambierol + 50 mM 1-BuOH). **E**, Bar chart shows the average reduction in current amplitude at +40 mV ± S.E.M. (obtained from recordings as shown in D, $n = 7$) after applying 50 mM 1-BuOH, 100 nM gambierol and the mixture gambi+1-BuOH. Fraction inhibition was calculated by normalizing the steady-state current in presence of drug/toxin to the current amplitude in control conditions. The expected inhibition according to an allotopic or syntopic model was calculated as described in the text. Note, the experimentally obtained inhibition with the mixture differed statistically (using paired t-tests) from the predicted value of either model (*, $p < 0.05$). **F**, Steady-state currents of *Shaker*-IR recorded upon sequential addition of 50 mM 1-BuOH, 3 mM 1-HeOH after washout of 1-BuOH, and the mixture 50 mM 1-BuOH + 3 mM 1-HeOH. **G**, Bar chart shows the fractional reduction in current amplitude at +40 mV ± S.E.M. ($n = 5$) after applying 50 mM 1-BuOH, 3 mM 1-HeOH and the mixture. The inhibition obtained with the mixture differed only statistically from the predicted value of an allotopic model (*, $p < 0.05$).

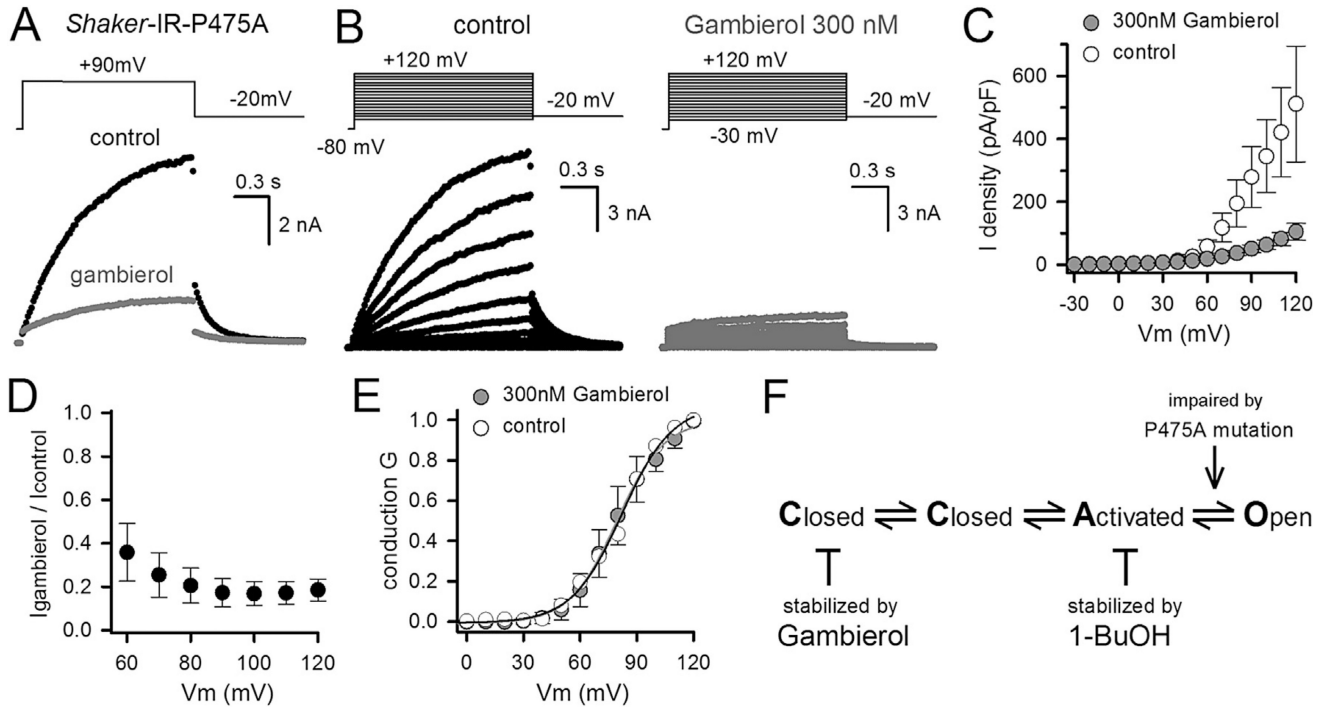

Fig. 2.

Inhibition of the *Shaker*-IR-P475A mutant by gambierol. **A**, Ionic currents of *Shaker*-IR-P475A, elicited using the pulse protocol shown on top, in control conditions (black trace) and after steady-state inhibition by 300 nM gambierol (gray trace). **B**, Representative family of currents of *Shaker*-IR-P475A recorded in control conditions (left) and in presence of 300 nM gambierol (right), elicited using the pulse protocol shown on top. **C**, Current density versus voltage relationship obtained by normalizing the peak current amplitude (from pulse protocols shown in panel B) to the cell capacitance, in control conditions (white circles, n = 4) and presence of 300 nM gambierol (gray circles). **D**, Lack of voltage dependence of gambierol inhibition: illustrated by relative suppression of currents at different potentials. The current suppression at +60 mV was not statistical different from that at +120 mV ($p > 0.1$). **E**, Normalized GV curves of *Shaker*-IR-P475A obtained in control conditions (white circles) and presence of 300 nM gambierol (gray circles). GV curves were obtained by plotting the normalized tail current amplitudes of recordings shown in panel B as a function of prepulse depolarization. Solid line represents the average fit with a single Boltzmann equation ($y = 1/\{1 + \exp[-(V - V_{1/2})/k]\}$). GV curves displayed a midpoint potential $V_{1/2}$ of 79 ± 1 mV (n = 4) and 82 ± 2 mV, and a slope factor k of 12.4 ± 0.8 mV and 13.2 ± 1.0 mV for control conditions and presence of 300 nM gambierol, respectively. **F**, A 4-state activation sequence of *Shaker* channels with two closed, one activated and an open state. Whereas gambierol locks the channels in the closed state, 1-BuOH stabilizes the activated state. The transition from this activated to open conformation is affected by the P475A pore mutation.